Effects of flavor-symmetry violation from staggered fermion lattice simulations of graphene

Joel Giedt,[1,*] Andrew Skinner,[2,1,†] and Saroj Nayak[1,‡]

[1]*Department of Physics, Applied Physics, and Astronomy, Rensselaer Polytechnic Institute, 110 Eighth Street, Troy, New York 12180-3590, USA*

[2]*Physics Department, Skidmore College, 815 North Broadway, Saratoga Springs, New York 12866, USA*

(Received 9 December 2009; revised manuscript received 1 December 2010; published 27 January 2011)

We analyze the effects of flavor splitting from staggered fermion lattice simulations of a low-energy effective theory for graphene. Both the unimproved action and the tadpole-improved action with a Naik term show significant flavor-symmetry breaking in the spectrum of the Dirac operator. Note that this is true even in the vicinity of the second-order phase transition point where it has been argued that the flavor-symmetry breaking should be small due to the continuum limit being approached. We show that at weaker couplings the flavor splitting is drastically reduced by stout link smearing, while this mechanism is ineffective at the stronger couplings relevant to suspended graphene. We also measure the average plaquette and describe how it calls for a reinterpretation of previous lattice Monte Carlo simulation results, due to tadpole improvement. After taking into account these effects, we conclude that previous lattice simulations are possibly indicative of an insulating phase, although the effective number of light flavors could be effectively less than two due to the flavor-splitting effects. If that is true, then simulations with truly chiral fermions (such as overlap fermions) are needed in order to settle the question.

DOI: 10.1103/PhysRevB.83.045420 PACS number(s): 73.22.Pr, 11.15.Ha, 64.60.Ej

I. INTRODUCTION

Recently, a number of lattice Monte Carlo simulations of graphene and graphenelike systems have appeared.[1–4] Refs. 1–3 study the effective theory of N_f flavors of massless four component Dirac fermions, constrained to $2+1$ dimensions, subject to an instantaneous $3+1$ dimensional Coulomb interaction.[5,6] In Ref. 4, a $2+1$-dimensional Thirring-like model is investigated. This is related to graphenelike systems through a large N_f or strong coupling equivalence in the dispersion relation for the auxiliary boson versus photon. Graphene has $N_f = 2$, but studying other N_f is of interest in order to understand the phases of such theories more generally, and because the large N_f limit is under theoretical control.[6] Other interesting studies coming from the effective field theory perspective have also recently appeared.[7,8]

In this paper we address the flavor-symmetry breaking that is introduced when staggered fermions are used in the lattice formulation. We also discuss the effect of photon tadpoles that come from lattice field theory. We will show that both features play an important role in the interpretation of lattice results. We explore various improvements to the lattice formulation. One is adding a Naik term to the action, which reduces discretization errors from $\mathcal{O}(a)$ to $\mathcal{O}(a^2)$, where a is the lattice spacing. Another is tadpole improvement, which removes ultraviolet divergent renormalizations associated with the lattice link operators. A final improvement that we consider is stout link smearing, which we find restores flavor symmetries at weak couplings but not at the strong couplings relevant to suspended graphene. Importantly, we find that flavor-symmetry breaking is significant in the vicinity of the second-order phase transition point that occurs in the noncompact gauge formulation. Thus, although it has been argued[3] that the continuum limit should be approached at this point, and hence flavor-symmetry violations [which are $\mathcal{O}(a)$] should be small in this regime, we have empirical results which contradict this expectation. Finally, we discuss how the flavor-symmetry violations, revealed in split eigenvalues of the Dirac operator spectrum, perhaps imply that there are effectively less light flavors than two. Given the phase diagram that has been suggested by a number of studies in the N_f versus inverse coupling plane, this would imply that the critical coupling for $N_f = 2$ would occur at a somewhat stronger coupling than is found from staggered fermions. Only a simulation with truly chiral lattice fermions, such as overlap (Neuberger) fermions,[9] can conclusively answer the question of what is the critical coupling for $N_f = 2$, since no systematic way of restoring the flavor symmetry has been found so far for the staggered fermion formulations at the stronger values of couplings.

The outline of this paper is as follows. In Sec. II we describe the action of the continuum effective theory that is supposed to describe the low-energy limit of suspended graphene. We pay particular attention to redefinitions that are involved in going to the action in its simplest form, as these will be mirrored in redefinitions made in the lattice formulation. It will be shown that in the massless limit there is only one parameter in the theory, a coupling g which is strong in the case of suspended graphene. We also describe the $U(4)$ flavor symmetry of the effective theory, which is spontaneously broken to $U(2) \times U(2)$ by the formation of a chiral condensate, when the coupling g is sufficiently strong. In Sec. III we discretize the continuum action, formulating the lattice theory with staggered fermions. We show the redefinitions that isolate the one parameter of the lattice theory (in the massless limit), $\beta = 1/g^2$. It is important here that we make redefinitions that maintain the unitarity of links; i.e., $U(n) = \exp[i\theta(n)]$, where $\theta(n)$ is a real lattice field representing the scalar potential associated with the instantaneous Coulomb interaction. Interestingly, this approach demands an anisotropic lattice with lattice spacing a_t in the time direction and a_s in the spatial directions, with the anisotropy parameter a_s/a_t set equal to the Fermi speed, $a_s/a_t = v_F$. Flavor symmetry violation of the unimproved staggered fermion formulation is discussed in Sec. IV. For $2+1$-dimensional staggered fermions, $\mathcal{O}(a_s, a_t)$ terms reduce the $U(4)$ flavor symmetry to $U(1) \times U(1)$ in the massless limit. We evaluate the spectrum of the unimproved Dirac operator

on a large number of lattice field configurations that we have generated by Monte Carlo techniques. We show that at stronger values of the coupling g (equivalent to small values of β), the flavor-symmetry violation is severe. This is revealed by the lack of fourfold spectrum degeneracies that would be present if the $U(4)$ symmetry were respected. We find that this is even true near the second-order phase transition point of the noncompact gauge formulation.

Section V describes Naik fermion and tadpole improvements to the lattice formulation. We do not find any restoration of flavor degeneracy but do find significant reinterpretation of the bare lattice parameters in terms of those that are tadpole improved, at strong coupling. It will be seen that that has important implications for the phase diagram of the theory. We measure the average plaquette in dynamical simulations. We will show that for stronger couplings the resulting tadpole improvement of the theory has a large effect when relating the simulation lattice coupling β to the coupling in the tadpole-improved action, $\beta_{\rm TI}$. The result is that for the noncompact gauge action the insulator/semimetal transition occurs at a physical coupling that is significantly smaller than the g^2 of suspended graphene. The apparent absence of a spectral gap in the experimental results for suspended graphene near the Dirac K points[10] is in conflict with the lattice simulations, and we will not be able to provide an explanation for this discrepancy.

The topic of stout link smearing, which is also a type of improvement, is discussed in Sec. VI. We find that this is very effective at weak couplings, but that it is not useful for restoring flavor symmetry at the strong coupling relevant to either graphene or the second-order phase transition point that occurs in the noncompact gauge action. We conclude in Sec. VII with a number of observations, summarizing our finding.

II. CONTINUUM ACTION

A. The effective coupling g

The Euclidean space-time action for the effective theory is given by

$$S = \int dt\, d^2x \sum_{\alpha=1,2} \Bigg(\bar\psi_\alpha \gamma_0 D_t \psi_\alpha + \hbar v_F \sum_{i=1,2} \bar\psi_\alpha \gamma_i \partial_i \psi_\alpha + mc^2 \bar\psi_\alpha \psi_\alpha \Bigg) + \frac{\epsilon_0}{2} \int dt\, d^3x \sum_{i=1}^{3} (\partial_i A_0)^2. \quad (1)$$

Here γ_i, $i = 0,1,2$, are Euclidean Dirac matrices satisfying the SO(3) Euclidean rotation group Clifford algebra $\{\gamma_i,\gamma_j\} = 2\delta_{ij}$. For instance, we could choose

$$\gamma_i = \begin{pmatrix} 0 & i\sigma_i \\ -i\sigma_i & 0 \end{pmatrix}, \quad i = 0,1,2, \quad (2)$$

composed of Pauli matrices with $\sigma_0 \equiv \sigma_3$. Also note that due to the nonrelativistic approximation, the covariant derivative only involves the scalar potential A_0,

$$D_t \equiv \hbar\partial_t - ieA_0. \quad (3)$$

Next we make the redefinitions

$$x_0 = v_F t, \quad A_0 = \frac{\hbar v_F}{e} A_0', \quad D_0 = \partial_0 - iA_0' \quad (4)$$

to obtain

$$\frac{1}{\hbar} S = \int d^3x \sum_{\alpha=1,2} \Bigg(\bar\psi_\alpha \gamma_0 D_0 \psi_\alpha + \sum_{i=1,2} \bar\psi_\alpha \gamma_i \partial_i \psi_\alpha + \frac{mc^2}{\hbar v_F} \bar\psi_\alpha \psi_\alpha \Bigg) + \frac{\epsilon_0 \hbar v_F}{2e^2} \int d^4x \sum_{i=1}^{3} (\partial_i A_0')^2. \quad (5)$$

Recall that the Euclidean path integral that defines the theory has as its integrand $\exp(-S/\hbar)$. The rescalings have isolated the sole coupling constant in the theory,

$$g^2 \equiv \frac{e^2}{\hbar v_F \epsilon_0} = (c/v_F) 4\pi\alpha, \quad (6)$$

where α is the fine structure constant. A final redefinition

$$A_0' = g\tilde A_0, \quad \tilde D_0 = \partial_0 - ig\tilde A_0 \quad (7)$$

makes it clear that g is the coupling constant in the photon-electron-electron vertex of this theory.

Perturbation theory would be valid in the limit where $\alpha_g \equiv \frac{g^2}{4\pi} = \alpha c/v_F \ll 1$, which is clearly not the case for graphene, where $c/v_F \approx 300$. Given that the coupling is in fact strong, it is natural to appeal to lattice Monte Carlo methods, as has been done in the case of the nuclear strong interaction, quantum chromodynamics (QCD). It also becomes clear why one would like to be able to adjust v_F experimentally, since the coupling of the theory determines the binding energy of any possible bound states that might form from the massless quasiparticles, analogous to hadrons in QCD. In fact, Refs. 1–4 argue that the theory is quite similar to QCD in that when the coupling is strong enough, one creates a nonzero chiral condensate $\langle \bar\psi_\alpha \psi_\beta \rangle \neq 0$, so that the theory is in a Mott insulator phase. (Properly speaking, chirality does not exist in $2+1$ dimensions. It is, rather, a flavor symmetry that is being spontaneously broken in the $2+1$-dimensional effective theory.)

B. Symmetries

The three-dimensional SO(3) $\simeq$ SU(2) rotation group acting on the spinors has generators $S_{ij} = \frac{1}{2}\sigma_{ij} \otimes \mathbf{1}$, where

$$\sigma_{ij} = -(i/2)[\gamma_i,\gamma_j] = \epsilon_{ijk}\ \mathrm{diag}\,(\sigma_k,\sigma_k) \quad (8)$$

and the $\mathbf{1}$ factor in $\frac{1}{2}\sigma_{ij} \otimes \mathbf{1}$ acts on the two-dimensional flavor space. The action (2) has a $U(4)$ flavor symmetry, with 16 generators that commute with those of the rotation group, Eq. (8):

$$\mathbf{1}\otimes\mathbf{1}, \quad \mathbf{1}\otimes\sigma_i, \quad \gamma_4\gamma_5\otimes\mathbf{1}, \quad \gamma_4\gamma_5\otimes\sigma_i, \quad (9)$$

$$\gamma_4\otimes\mathbf{1}, \quad \gamma_4\otimes\sigma_i, \quad \gamma_5\otimes\mathbf{1}, \quad \gamma_5\otimes\sigma_i, \quad (10)$$

where $\gamma_{4,5}$ are given by

$$\gamma_4 = \begin{pmatrix} 0 & 1 \\ 1 & 0 \end{pmatrix}, \qquad \gamma_5 = \begin{pmatrix} -1 & 0 \\ 0 & 1 \end{pmatrix} \quad (11)$$

when we choose the Dirac matrices (2). A mass term $m\sum_\alpha \bar\psi_\alpha\psi_\alpha$ reduces the symmetry to $U(2)\otimes U(2)$ since the generators (10) are broken. However, we still expect a fourfold

degeneracy in the spectrum of the Dirac operator

$$M = \gamma_0 D_0 + \sum_{i=1,2} \gamma_i \partial_i + \frac{mc^2}{\hbar v_F} \tag{12}$$

because the **4** representation of $U(4)$ decomposes to a $(\mathbf{2},\mathbf{2})$ representation of the subgroup $\mathrm{SU}(2) \otimes \mathrm{SU}(2)$. [In spin language, this is the $(j_1, j_2) = (1/2, 1/2)$ representation of $\mathrm{SU}(2)_1 \otimes \mathrm{SU}(2)_2$.] This is important in our considerations below because the Monte Carlo simulations are done at a nonzero mass, in order to avoid numerical difficulties (inversion of a poorly conditioned Dirac matrix). We will examine the spectrum of the Dirac operator on the lattice and compare to this fourfold degeneracy of the continuum theory with a mass term.

The formation of a chiral condensate $\langle \bar{\psi}_\alpha \psi_\beta \rangle \neq 0$ in the $m \to 0$ limit would signal a spontaneous breaking of the $U(4)$ symmetry. In the case $\langle \bar{\psi}_\alpha \psi_\beta \rangle \propto \delta_{\alpha\beta}$ the symmetry is reduced to $U(2) \otimes U(2)$, and in the massless limit $m \to 0$ there will be eight massless Goldstone pseudoscalar modes, parametrizing the coset $U(4)/U(2) \otimes U(2)$, with a low-energy dynamics described by the corresponding chiral perturbation theory. The formation of the chiral condensate requires a sufficiently strong value of g, so there is a phase boundary at which the condensation "turns on." The works[1–4] have located this phase boundary using lattice Monte Carlo methods.

III. DISCRETIZATION

The fermionic part of the action (1) is easily discretized using the staggered fermion formulation.[11] The gauge-field part of the action can be discretized in two ways, compact and noncompact, both of which will be described and used here. From this point on, we work in units where $\hbar = c = 1$, and use a lattice spacing a_t in the time direction and a_s in the spatial directions. Thus we have lattice fields at the sites $t = a_t n_0$, $x_i = a_s n_i$ $(i = 1,2,3)$, where $n_0, \ldots, n_3$ are integers. We are permitting $a_s \neq a_t$ because the anisotropy parameter a_s/a_t will provide us with the handle to remove the Fermi velocity v_F from the lattice action, so that the only parameters that will appear are the coupling (6) and the fermion mass (which must eventually be taken to zero). This mirrors the continuum redefinition $x_0 = v_F t$ which appears in Eq. (4). The lattice action takes the form

$$S = \frac{1}{2} \sum_{n_0 n_1 n_2} a_t a_s^2 \left\{ \frac{1}{a_t} [\bar{\chi}(n) U(n) \chi(n+\hat{0}) - \bar{\chi}(n) U(n-\hat{0}) \chi(n-\hat{0})] \right.$$
$$\left. + v_F \frac{1}{a_s} \sum_{i=1}^{2} \eta_i(n) [\bar{\chi}(n) \chi(n+\hat{\imath}) - \bar{\chi}(n) \chi(n-\hat{\imath})] + m \bar{\chi}(n) \chi(n) \right\} + \sum_{n_0 \cdots n_3} a_t a_s^3 \frac{\epsilon_0}{2} \sum_{i=1}^{3} \left(\frac{\theta(n) - \theta(n-\hat{\imath})}{a_s} \right)^2 . \tag{13}$$

The notation employs four-vectors $n = (n_0, n_1, n_2, n_3)$ and unit vectors $\hat{0} = (1,0,0,0)$, etc. Here $\chi, \bar{\chi}$ are one-component fermions and as site-dependent coefficients one has the staggered phase factors $\eta_1(n) = (-1)^{n_0}$ and $\eta_2(n) = (-1)^{n_0+n_1}$. The reason that one-component fermions can be used is because staggered fermions "suffer" from doubling, so that in three dimensions there are eight continuum modes, which organize themselves into two four-component fermions under a change of basis.[12] The link fields are defined as $U(n) = \exp[iea_t\theta(n)]$, where $\theta(n)$ is the lattice version of the scalar potential $A_0(x)$. Here we have used the noncompact form of the gauge action in the last term. The compact form will be discussed at a later point below.

We next rescale to dimensionless fields, $\chi \to \chi/a_s$ and $\theta \to \theta/a_t e$ to obtain

$$S = \frac{1}{2} \sum_{n_0 n_1 n_2} \left\{ \bar{\chi}(n) U(n) \chi(n+\hat{0}) - \bar{\chi}(n) U(n-\hat{0}) \chi(n-\hat{0}) \right.$$
$$+ v_F \frac{a_t}{a_s} \sum_{i=1}^{2} \eta_i(n) [\bar{\chi}(n) \chi(n+\hat{\imath}) - \bar{\chi}(n) \chi(n-\hat{\imath})]$$
$$\left. + m a_t \bar{\chi}(n) \chi(n) \right\} + \sum_{n_0 \cdots n_3} \frac{a_s}{a_t} \frac{\epsilon_0}{2} \sum_{i=1}^{3} [\theta(n) - \theta(n-\hat{\imath})]^2 . \tag{14}$$

Finally, we can absorb the Fermi speed v_F into the anisotropy parameter, choosing $a_s/a_t = v_F$, to obtain the lattice action in its most convenient form,

$$S = \frac{1}{2} \sum_{n_0 n_1 n_2} \left\{ \bar{\chi}(n) U(n) \chi(n+\hat{0}) - \bar{\chi}(n) U(n-\hat{0}) \chi(n-\hat{0}) \right.$$
$$+ \sum_{i=1}^{2} \eta_i(n) [\bar{\chi}(n) \chi(n+\hat{\imath}) - \bar{\chi}(n) \chi(n-\hat{\imath})]$$
$$\left. + \hat{m} \bar{\chi}(n) \chi(n) \right\} + \sum_{n_0 \cdots n_3} \frac{\beta}{2} \sum_{i=1}^{3} [\theta(n) - \theta(n-\hat{\imath})]^2, \tag{15}$$

where

$$\beta = \frac{1}{g^2} = \frac{v_F \epsilon_0}{e^2}, \quad \hat{m} = m a_t. \tag{16}$$

A slightly different choice for the anisotropy parameter a_s/a_t will be made below when we come to tadpole improvement.

We also consider the case of a compact gauge action, where the last term in Eq. (15) is replaced by

$$-\beta \sum_{n_0 \cdots n_3} \sum_{i=1}^{3} \mathrm{Re}\ U(n) U^*(n-\hat{\imath}). \tag{17}$$

In the weak-field limit [small $\theta(n)$], which corresponds to large β, the two formulations are equivalent. However, at small β it is expected that there will be qualitative differences.

IV. FLAVOR-SYMMETRY VIOLATION

As previously stated, a single staggered fermion automatically yields two flavors, as the staggered formulation does not fully solve the doubling problem. In the continuum, the massless theory with two flavors has a $U(4)$ flavor symmetry, which is reflected in a degeneracy of the spectrum of the Dirac operator. On the other hand, it is known that the leading order spectral degeneracies of the lattice Dirac operator are broken by flavor violating higher-order terms (in the lattice spacings a_t, a_s). In the massless limit but at nonzero lattice spacing, only a $U(1) \otimes U(1)$ flavor symmetry remains (in addition to some discrete symmetries).[13] Long ago it was shown in the $3+1$-dimensional case that the flavor-symmetry breaking can be seen by going to the "flavor basis."[14] For $2+1$ dimensions, see, for example, Ref. 15, where staggered fermion flavor-breaking terms were previously considered in the context of the Thirring model. Thus in the present paper we are reiterating concerns that were already raised in Ref. 15, though here our principal concern is the effect in the context of graphene effective lattice field theory. Although the flavor-symmetry breaking terms are irrelevant operators (i.e., they are suppressed by a_t, a_s), at one loop and at finite lattice spacing they have important effects on the self-energy of the fermions.[13] The effect of this flavor-symmetry violation on the order parameter $\langle \bar{\psi}\psi \rangle$ that is used to distinguish the semimetal versus insulator phases is not known, though in our Conclusions we will make a conjecture for what might occur. The flavor-changing interactions are a lattice artifact that is known to disappear in the continuum limit. Hence, if one could send the lattice spacings a_t, a_s of the discretized effective theory (not to be confused with the lattice constant of the graphene system itself) to zero, one would recover the full $U(4)$ symmetry.[13] However, the Monte Carlo simulations are performed at finite a_t, a_s, and so this lattice artifact must be taken into account. Thus it is not quite accurate to say that one is simulating the effective theory with two $(1+3)$-dimensional Dirac fermions constrained to a plane, equivalent to four massless $(1+2)$-dimensional Dirac fermions. An extrapolation in the lattice spacing or suppression of the lattice artifacts is needed. One would like a systematic way to remove these lattice artifacts. This motivates the present study.

We determine the size of the flavor splitting by studying the eigenvalues of the lattice Dirac operator, which is the discretization of Eq. (12) corresponding to the lattice action (15). In Fig. 1 the "unimproved" data shows the average spectrum of the staggered Dirac operator, for the lowest-lying modes. Here a Monte Carlo simulation was performed with $\beta = 0.11$, and eigenvalues were obtained for each configuration of the gauge field. The error bars in the figure indicate the standard deviation in the eigenvalues. It can be seen that there is a linear rise in eigenvalues, with no degeneracies whatsoever. Thus at strong coupling the flavor symmetry of the continuum is badly broken.

Next we consider the case of weak coupling, $\beta = 4.0$. In Fig. 3 the unimproved data shows evidence of approximate degeneracies. The weaker coupling leads to smoother configurations of the gauge field. Rough gauge fields are farther away from the continuum limit, so that the $\mathcal{O}(a_t, a_s)$ flavor-symmetry violation (FSV) is more pronounced.

We have examined the spectrum for other values of β. The general pattern is that for strong coupling the flavor symmetry is badly broken. Our next task is to attempt to restore it, since the β corresponding to graphene and the phase transition of the effective theory is at a strong coupling value.

V. IMPROVEMENT

Some time ago the lattice QCD community set aside unimproved staggered fermions due to unwanted lattice artifacts. Modern staggered fermions are improved in various ways in order to suppress these effects.[16,17] So-called AsqTad staggered fermions were popular for several years for the study of K and B physics (e.g., Ref. 18). Further improvements have been introduced to produce highly improved staggered quarks (HISQ) staggered fermions.[19] Detailed studies of the low-lying eigenvalue spectrum of various staggered Dirac operators have, for instance, been conducted in Ref. 20. In each case, an important effect is to restore the flavor degeneracy by suppressing flavor-changing interactions. The present work represents a first attempt in that direction; however, we will find that improvement of staggered fermions in the present context is more difficult. The reason is that for the study of graphene and the phase transition of the effective theory the coupling is strong, where the flavor symmetry is badly broken.

In lattice QCD it is known that flavor-symmetry breaking can be ameliorated by making improvements to the lattice action that reduce lattice artifacts. An expansion in the lattice spacing a (or a_t, a_s in our case) and gauge coupling g allows for coefficients of various improvement terms to be determined in perturbation theory. However, asymptotic freedom should be important, since in that case it is clear how one makes these coefficients small in matching onto the desired continuum theory. It is then an important question whether for the strongly coupled theory of graphene, where there is no asymptotic freedom, the lattice action can be improved so as to reduce the flavor-symmetry-breaking effects. Certainly perturbative improvement is out of the question.

A. Tadpole improvement

Tadpoles arise from $\langle A_0^2(x) \rangle \sim \langle \theta^2(n) \rangle \sim 1/a_t^2$, where the estimate is made on dimensional grounds. As previously mentioned, we study both the compact and noncompact gauge actions. In the noncompact case, gauge-field tadpoles only enter the perturbation series through the gauge links $U(n) = \exp[i a_t e \theta(n)]$ that are contained within the fermion action. In the compact case there are additional multiphoton vertices coming from expansion of the gauge action (17). Consider the following example in the fermion timelike hopping terms. In this, we reintroduce the dimensions and canonical kinetic term for $\theta(n)$ through $\theta(n) \to a_t g \theta(n)$. Then, expanding the link $U(n) = \exp[i a_t g \theta(n)]$ and focusing on the contribution to the fermion self-energy, we obtain a term $a_t g^2 \langle \theta^2(n) \rangle \bar{\chi}(n) \chi(n + \hat{0}) \sim (g^2/a_t) \bar{\chi}(n) \chi(n + \hat{0})$. That is, there is a large correction to the hopping term, even though the $\theta^2 \bar{\chi} \chi$ vertex is irrelevant by power counting. There is also a large effect on the marginal $\theta \bar{\chi} \chi$ vertex:

$$\begin{aligned} & i g \theta(n) 1 - \tfrac{1}{2} a_t^2 g^2 \langle \theta^2(n) \rangle + \cdots \bar{\chi}(n) \chi(n + \hat{0}) \\ & \quad = i g \theta(n) 1 + \mathcal{O}(g^2) \bar{\chi}(n) \chi(n + \hat{0}). \end{aligned} \tag{18}$$

Here again, the correction is $\mathcal{O}(g^2)$ rather than $\mathcal{O}(g^2 a_t^2)$, due to the tadpole $\langle \theta^2(n) \rangle \sim 1/a_t^2$. The tadpoles associated with the irrelevant fermion vertices thus give significant contributions

to the renormalization of g, causing the matching onto continuum perturbation theory to be problematic. This can be circumvented through a change in renormalization scheme, known as tadpole improvement.[21] In fact, since for graphene the value of g is large, the tadpole corrections are out of perturbative control and must be evaluated nonperturbatively.

We will now show that the translation between the bare lattice $\beta = 1/g^2$ (i.e., the parameter that appears in the action that is simulated) and its tadpole-improved value $\beta_{\rm TI}$ is somewhat different depending on whether the compact or noncompact form of the gauge action is used, more so at stronger values of the coupling. From this, the physical coupling—as estimated by the tadpole-improved value $\beta_{\rm TI}$—is different from the bare coupling, due to radiative effects. In fact, we will reproduce the results of Ref. 3 regarding the relationships between $\beta_{\rm TI}$ and β.

We begin with the expectation value $\langle P\rangle$ of the plaquette operator $P = U(n)U^*(n+\hat{\imath})$, $i = 1$ or 2, which is related to $\langle A_0^2(x)\rangle$. The average link u_0 is defined through this quantity:

$$u_0 = \langle P\rangle^{1/2}. \tag{19}$$

Note that the square root is used here, in contrast to the fourth root that appears in QCD applications, since the plaquette operator is quadratic in the links that are allowed to fluctuate in the present, nonrelativistic formulation.

Tadpole improvement[21] can be understood as integrating out ultraviolet modes of the link operator $U(x)$, to obtain an effective infrared link operator. The quantity u_0 represents the ultraviolet divergent effects of tadpoles $\langle A_0^2\rangle$. Thus, the link is related to an infrared (IR) field $V(n)$ or $\theta^{\rm IR}(n)$:

$$U(n) \equiv u_0 V(n) \approx u_0[1 + i a_t e\theta^{\rm IR}(n)]. \tag{20}$$

When the lattice is formulated using instead the $V(n) = U(n)/u_0$ links, one has

$$S = \sum_{n_0 n_1 n_2}\left\{\frac{a_s^2}{u_0}[\bar\chi(n)U(n)\chi(n+\hat 0) - \bar\chi(n)U(n-\hat 0)\chi(n-\hat 0)] + v_F a_t a_s\sum_{i=1}^{2}\eta_i(n)[\bar\chi(n)\chi(n+\hat\imath) - \bar\chi(n)\chi(n-\hat\imath)] + m a_t a_s^2\bar\chi(n)\chi(n)\right\} + \sum_{n_0\cdots n_3} a_t a_s\frac{\epsilon_0}{2}\sum_{i=1}^{3}[\theta(n) - \theta(n-\hat\imath)]^2. \tag{21}$$

The redefinition of variables is now

$$\chi = \frac{\sqrt{u_0}}{a_s}\chi', \quad \theta = \frac{1}{a_t e}\theta' \tag{22}$$

One finds that $a_s/a_t = v_F u_0$ simplifies the spatial derivative term and that the result is Eq. (15) except that β and $\hat m$ are replaced by

$$\beta = u_0\frac{v_F\epsilon_0}{e^2} = u_0\beta_{\rm TI}^{\rm nc}, \quad \hat m = u_0\hat m_{\rm TI}. \tag{23}$$

Note that $\beta_{\rm TI}^{\rm nc}$ and $\hat m_{\rm TI}$ are what would have appeared in the lattice action had we not included u_0 in the redefinition (22). Hence these are the inverse coupling and dimensionless mass of the tadpole-improved action. By contrast, β and $\hat m$ are the inverse coupling and mass that are used in the simulation after going to the redefined variables where the action takes its simplest form (i.e., u_0 does not appear explicitly). Thus in the massless limit, for the noncompact gauge action, the entire effect of the tadpole improvement is to rescale the inverse coupling according to this equation. Something similar occurs in the compact gauge action case. There we have, in addition, a factor $1/u_0^2$ in front of the gauge term,

$$\sum_{n_0\cdots n_3}\frac{1}{u_0^2}\frac{a_s}{a_t}\frac{\epsilon_0}{2e^2}\sum_{i=1}^{3}U(n)U^*(n+\hat\imath). \tag{24}$$

Here then the result is

$$\beta = \frac{1}{u_0}\beta_{\rm TI}^{c}. \tag{25}$$

These rescalings of β agree with those found recently in Ref. 3.

B. Naik improvement

The Naik[22] fermion action improvement reduces discretization errors and when the tadpole improvement is also performed it is given by

$$\begin{aligned} S_N = {} & a_s^2\sum_{n_0 n_1 n_2}\bar\chi(n)\frac{1}{2}\left\{\frac{c_1}{u_0}[U(n)\chi(n+\hat 0) - U^*(n-\hat 0)\chi(n-\hat 0)]\right. \\ & \left. + \frac{c_2}{u_0^3}[U(x)U(n+\hat 0)U(n+2\hat 0)\chi(n+3\hat 0) - U^*(n-\hat 0)U^*(n-2\hat 0)U^*(n-3\hat 0)\chi(n-3\hat 0)]\right\} \\ & + v_F a_s a_t\sum_{i,n_0 n_1 n_2}\eta_i(n)\bar\chi(n)\frac{1}{2}\{c_1[\chi(n+\hat\imath) - \chi(n-\hat\imath)] + c_2[\chi(n+3\hat\imath) - \chi(n-3\hat\imath)]\} + a_s^2 a_t m\sum_{n_0 n_1 n_2}\bar\chi(n)\chi(n). \end{aligned} \tag{26}$$

Tree-level improvement makes the action $\mathcal{O}(a^2)$ accurate by setting $c_1 = 9/8$ and $c_2 = -1/24$.

Next we make the redefinitions (22), together with setting $a_s/a_t = v_F u_0$ as before, to obtain

$$\begin{aligned} S_N = {} & \sum_{n_0 n_1 n_2}\bar\chi'(n)\frac{1}{2}\left\{c_1[U(n)\chi'(n+\hat 0) - U^*(n-\hat 0)\chi'(n-\hat 0)] + \frac{c_2}{u_0^2}[U(x)U(n+\hat 0)U(n+2\hat 0)\chi'(n+3\hat 0)\right. \\ & \left. - U^*(n-\hat 0)U^*(n-2\hat 0)U^*(n-3\hat 0)\chi'(n-3\hat 0)]\right\} \\ & + \sum_{i,n_0 n_1 n_2}\eta_i(n)\bar\chi'(n)\frac{1}{2}\{c_1[\chi'(n+\hat\imath) - \chi(n-\hat\imath)] + c_2[\chi'(n+3\hat\imath) - \chi'(n-3\hat\imath)]\} + \hat m\sum_{n_0 n_1 n_2}\bar\chi'(n)\chi'(n), \end{aligned} \tag{27}$$

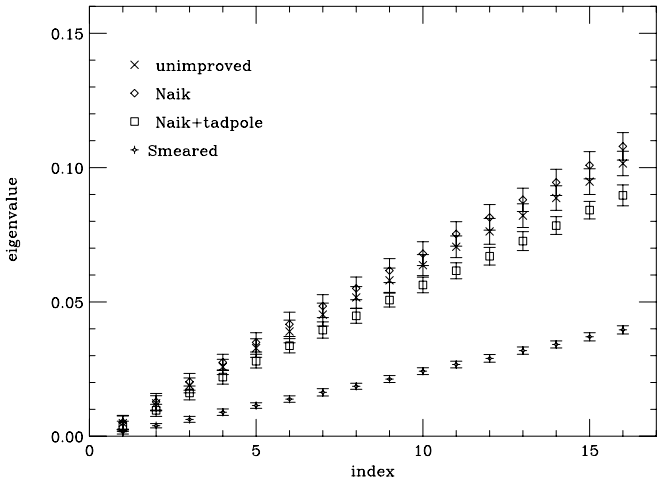

FIG. 1. Spectrum of lowest-lying modes of the three massless Dirac operators we consider, for compact gauge action. The configurations of gauge fields were dynamically generated at $\beta = 0.11$ and $m = 0.01$ on a $12^3 \times 8$ lattice with the unimproved staggered fermion action and plaquette gauge term. The tadpole improvement of the Naik Dirac operators used $u_0 = 0.256$. Average eigenvalues are shown, and the error bars represent standard deviations.

where again, $\hat{m} = ma_t u_0$. This is the "Naik-tadpole improvement"; note that u_0 appears explicitly in this action. To obtain just the Naik improvement, one can set $u_0 = 1$ in the previous expressions.

C. Spectrum results

We have computed the low-lying eigenvalues of the spectrum of the Dirac operator on dynamical configurations at various values of β, in order to see the size of the flavor-symmetry violating effect. Figure 1 shows the spectrum of average eigenvalues for $\beta = 0.11$, $\hat{m} = 0.01$ on $12^3 \times 8$ lattices, with compact gauge action, as well as the standard deviation (by error bars). Figure 2 shows the same thing except that the noncompact gauge action was used. In either case, one can see that there is no hint of the fourfold degeneracy of the continuum theory and that the splitting is of the order 0.02. By comparison, the explicit mass in the simulations of Ref. 1 ranged from 0.0025 to 0.02. Thus the flavor-changing interactions split the spectrum at the order of the mass or greater, and one is far from the desired theory. Since according the to Banks-Casher relation[23] the condensate on the lattice is determined by the density of near-zero modes, a significant systematic error will be introduced by the flavor splitting that we observe. We note that for the "improved" Dirac operators the splitting is not at all improved. This would seem to indicate that the lattice is actually quite coarse, so that suppressing lattice artifacts cannot be achieved by simple power counting in the lattice spacings a_t, a_s, such as is done in the Naik improvement. It is also worth mentioning that large scaling violations were seen in Ref. 1 for strong coupling (very small values of β) which would be a further indication that lattice artifacts are playing a dominant role. However, the fact that Ref. 1 observed scaling in a regime where we see large flavor violations is interesting, as it suggests that there is a universal description but that it is one with less flavor symmetry than the $U(4)$ of the target graphene effective theory.

As a further check, we have also computed the spectrum from a simulation at the weak coupling $\beta = 4$, where the flavor violation is expected to be small due to weak interactions. We also note that at this weak value of the coupling the compact and noncompact formulations of the gauge action are completely equivalent. Thus the flavor-symmetry breaking that we next describe is universal. At large β the fluctuations in the gauge-field strength are suppressed and a perturbative expansion of the link operators $U_0(x) \approx 1 + iagA_\mu(x)$ should be valid. Results for the low-lying eigenvalues of the three types of Dirac operators are shown in Figs. 3 and 4, and these certainly show a closer approximation to the fourfold degeneracy. However, the improved Dirac operators do not show any superiority to the unimproved one. This somewhat surprising result suggests that a further improvement may be needed, such as smearing, which is something we explore in the next section.

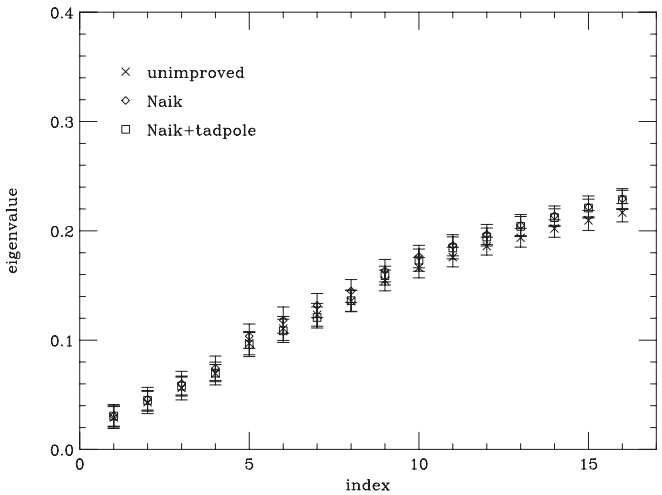

FIG. 2. Same as Fig. 1 except that here we use the noncompact gauge action.

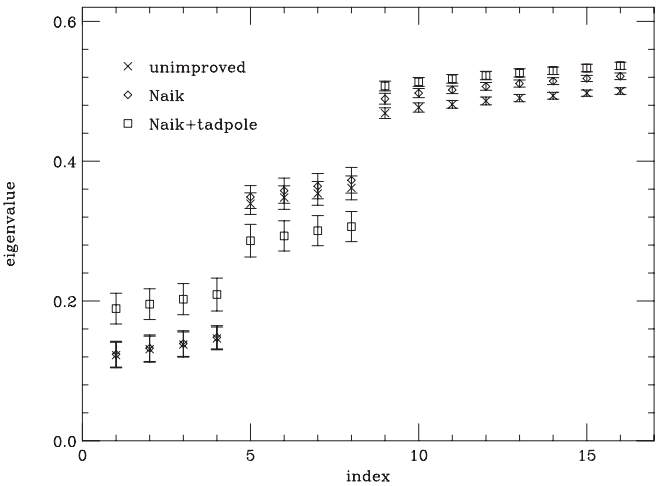

FIG. 3. Similar to Fig. 1 (compact gauge action) except that $\beta = 4.0$ and $u_0 = 0.974$.

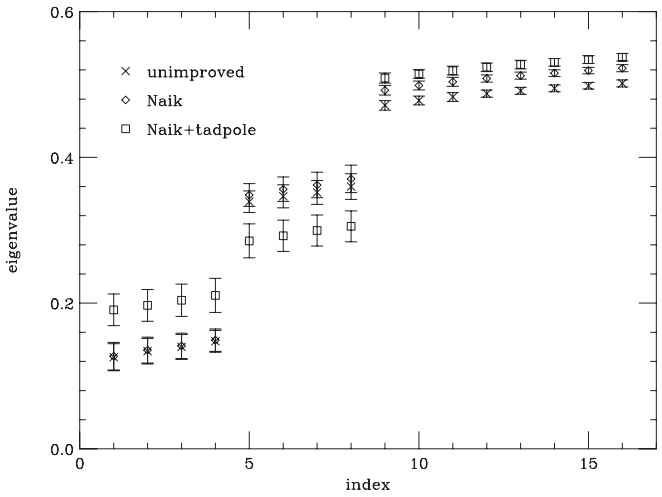

FIG. 4. Similar to Fig. 2 (noncompact gauge action) except that $\beta = 4.0$ and $u_0 = 0.974$.

It is also interesting to have a statistical measure for what happens to flavor symmetry over an ensemble. For this purpose we have computed

$$R_{\mathrm{FSV}} = \frac{\bar{\lambda}_4 - \bar{\lambda}_1}{\frac{1}{4}(\bar{\lambda}_1 + \bar{\lambda}_2 + \bar{\lambda}_3 + \bar{\lambda}_4)}, \tag{28}$$

where $\bar{\lambda}_i$ is the average value of the ith eigenvalue. This measures the relative flavor-symmetry breaking in the first four eigenvalues. On the $\beta = 0.11$ (compact) lattice we obtain $R_{\mathrm{FSV}} \approx 1.4(1)$. On the $\beta = 4.0$ (compact) lattice we obtain $R_{\mathrm{FSV}} \approx 0.18(2)$. These results are independent of the improvement, which is curious at the larger β.

D. Relation between β's

Previously, we found that the value of β_{TI} in the tadpole-improved action can be related to another value β obtained after redefinitions, given by Eqs. (23) and (25). The latter should be used in the simulation with an action that is equivalent to one without tadpole improvement (or only a factor $1/u_0^2$ on the temporal Naik term). We are therefore interested in the effective value β_{TI} as a function of β so that we know how to interpret simulations done at β in terms of the underlying β_{TI}. For instance, Drut and Lähde find a critical value of the coupling for which a condensate forms, and this should be interpreted as a value of β at which the simulation is done (i.e., in an action without u_0 appearing explicitly). To see what this physically corresponds to, one must translate back to $\beta_{\mathrm{TI}}^{\mathrm{nc}}$ in order to find the value of the coupling in the tadpole-improved action, where ultraviolet artifacts are minimized.

Results for the compact and noncompact actions are summarized in Tables I and II, respectively. Thus to simulate graphene, which has $\beta_{\mathrm{TI}} \approx 0.037$, we should choose the modified values β given in the first rows of Tables I or II, depending on the form of the gauge action. This gives $\beta \approx 0.12$ for compact and $\beta \approx 0.004$ for noncompact gauge actions. The simulation coupling where Drut and Lähde have found a phase transition is $\beta_c \approx 0.074$. The physical value of the inverse coupling is then approximately $\beta_{\mathrm{TI}}^{\mathrm{nc}} \approx 0.21$, which is at a coupling significantly weaker than graphene, $\beta_{\mathrm{TI}} \approx 0.037$. Thus the appearance of the condensate $\langle\bar{\psi}\psi\rangle$ occurs for a weaker value of the coupling, and will persist at the stronger value of graphene. One concludes that the lattice simulation is indicative of an insulator phase. This is in agreement with the findings of Ref. 3.

TABLE I. The average plaquette $\langle P\rangle$ and the tadpole correction factor u_0 that is derived from it, as a function of β, for the compact gauge action. This then gives a value for tadpole-improved inverse coupling $\beta = \beta_{\mathrm{TI}}^{\mathrm{c}}$. For instance, for graphene we want $\beta_{\mathrm{TI}}^{\mathrm{c}} = 0.037$ and the inverse coupling that should be used in the simulation is $\beta \approx 0.12$.

β	$\langle P\rangle$	u_0	$\beta_{\mathrm{TI}}^{\mathrm{c}}$
0.037	0.0306(40)	0.175(11)	0.006 47(42)
0.058	0.034(3)	0.183(7)	0.010 61(41)
0.11	0.066(4)	0.256(8)	0.028 16(88)
0.15	0.0901(44)	0.3002(73)	0.0450(11)
0.25	0.1492(43)	0.3863(56)	0.0965(15)
0.5	0.504(6)	0.710(4)	0.355(2)
1.0	0.814(3)	0.9023(14)	0.9023(14)
2.0	0.9120(13)	0.9550(7)	1.91(14)
4.0	0.949(2)	0.974(1)	3.896(4)

We also mention in passing that the value of $\langle P\rangle$ and hence u_0 turned out to be essentially independent of which fermion action (unimproved, Naik-improved, or Naik-tadpole-improved) we used in the simulation. We also changed the mass to 0.02 and find the same value of u_0.

VI. STOUT LINK SMEARING

We have seen that at weak coupling (large β), the spectrum degeneracies start to appear. This is the result of the fact that in this regime the gauge fields are smooth, whereas at strong coupling the gauge fields are rough. Clearly what is needed at strong coupling is a way to smooth out the short-distance (unphysical) roughness without destroying the long-distance

TABLE II. The average plaquette $\langle P\rangle$ and the tadpole correction factor u_0 that is derived from it, as a function of β, for the noncompact gauge action. This then gives a value for tadpole-improved inverse coupling $\beta = \beta_{\mathrm{TI}}^{\mathrm{nc}}$. For instance, for graphene $\beta_{\mathrm{TI}}^{\mathrm{nc}} = 0.037$, and the inverse coupling that should be used in the simulation is $\beta \approx 0.004$.

β	$\langle P\rangle$	u_0	$\beta_{\mathrm{TI}}^{\mathrm{nc}}$
0.002	0.0131(37)	0.114(16)	0.0175(25)
0.004	0.0108(54)	0.104(26)	0.0385(96)
0.005	0.0121(41)	0.110(19)	0.0455(78)
0.01	0.0121(27)	0.110(12)	0.091(10)
0.02	0.0118(42)	0.108(19)	0.184(33)
0.037	0.0272(46)	0.165(14)	0.224(19)
0.058	0.0757(40)	0.2751(73)	0.2108(56)
0.11	0.2392(45)	0.4891(46)	0.2249(21)
0.25	0.5228(40)	0.7230(27)	0.3458(13)
0.5	0.7192(29)	0.8481(17)	0.5896(12)
1.0	0.8466(20)	0.9201(11)	1.0868(13)
2.0	0.9195(11)	0.9589(6)	2.0857(13)
4.0	0.94(2)	0.97(1)	4.124(43)

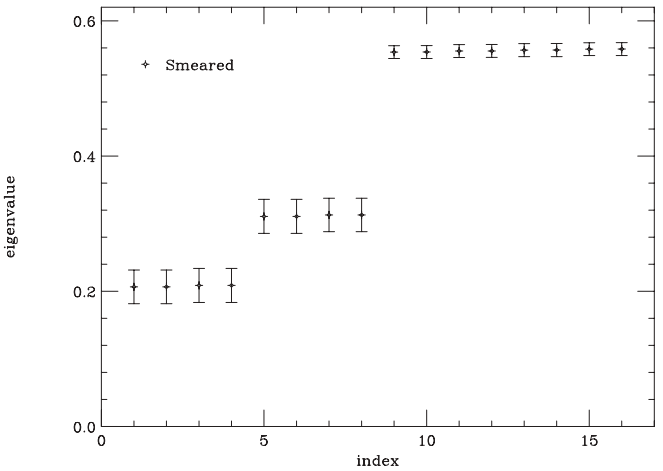

FIG. 5. $\beta = 4.0$, compact gauge action, ten stout link smearings with $\rho = 1/6$.

(physical) fluctuations of the gauge field. The way that this can be done is to use smeared links in the fermion action. Here we will study stout link smearing[24] and will find that it successfully restores the level degeneracies for moderate to weak coupling, but that it fails at couplings as strong as graphene, $\beta_{\rm TI} = 0.037$.

Stout link smearing in the present context introduces the definitions

$$C(n) = \rho \sum_{i=1}^{3} [U(n+\hat{\imath}) + U(n-\hat{\imath})], \quad \Omega(n) = C(n)U^*(n),$$
$$Q(x) = \frac{i}{2}[\Omega^*(n) - \Omega(n)], \tag{29}$$

and $U^{(k)}(n)$ at smearing step k are mapped into $U^{(k+1)}(n)$ according to

$$U^{(k+1)}(n) = \exp[i\,Q^{(k)}(n)]U^{(k)}(n). \tag{30}$$

It can be seen in Fig. 5 that smearing works very well at weak coupling. The smeared eigenvalue data has ten smearing iterations with smearing parameter $\rho = 1/6$, where the latter

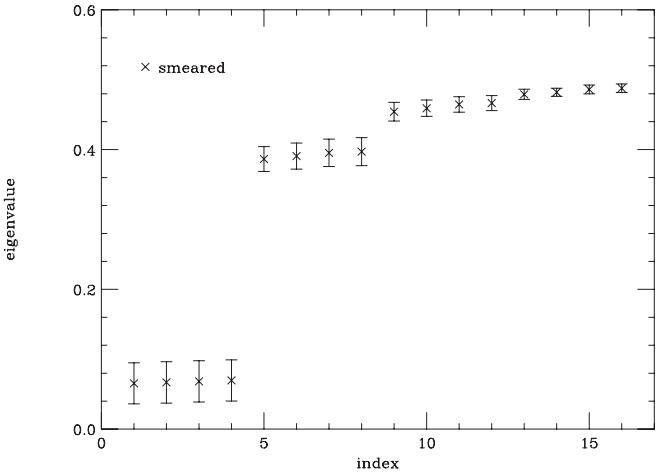

FIG. 6. $\beta = 0.11$, noncompact gauge action, ten stout link smearings with $\rho = 1/6$.

was found to be optimal based on trial and error. Less smearing iterations obviously results in less degeneracy. Unfortunately, as the coupling is made stronger, the smearing becomes progressively less effective, as can be seen in Fig. 1.

By contrast for the noncompact gauge action, even at the relatively small value of $\beta = 0.11$, one finds a significant improvement from smearing (see Fig. 6). Since the phase transition occurs at $\beta \approx 0.07$ we expect smearing to be quite useful for reducing flavor-symmetry breaking in the vicinity of this point. On the other hand, from Table II we found that graphene with $\beta_{\rm TI}^{\rm nc} = 0.037$ corresponds to $\beta \approx 0.004$, which is far too strong for smearing to help. Indeed we have found that there is no restoration of degeneracy in this case.

VII. CONCLUSIONS

We have found that at $\beta \lesssim 1$ both the unimproved action, and the tadpole-improved action with a Naik term show significant flavor-symmetry breaking. We have also measured the average plaquette term used for tadpole improvement and have described how it calls for a reinterpretation of previous lattice simulation results. Importantly, it indicates that the insulator/semimetal phase transition observed on the lattice occurs at a physical coupling that is significantly weaker than the one that appears in suspended graphene. It follows that the lattice simulations predict that the chiral symmetry is spontaneously broken and that suspended graphene would be in the insulating phase.

On the other hand, conjectured phase diagrams in the g versus N_f plane would indicate that the critical g decreases as N_f is decreased. So, if the staggered formulation really simulates effectively less than $N_f = 2$ due to the flavor-symmetry breaking, the lattice simulations would predict a critical g that is weaker than that of graphene. Restoration of the $U(2N_f)$ flavor symmetry would tend to increase the value of the critical g. Thus it is still possible, though unlikely, that lattice simulations would predict that suspended graphene is in the semimetal phase, provided the full flavor symmetry is intact. We think that it is unlikely since the critical β_c would have to shift all the way from $\beta = 0.07$ to $\beta = 0.004$ as a result of restoring the flavor symmetries. Still, a study with overlap fermions is of interest to settle the question.

We have conducted studies with both the compact and noncompact formulations in their gauge action. In $1+3$-dimensional quantum electrodynamics, the compact formulation has difficulties with a bulk phase transition in the strong-coupling regime, separating it from the continuum theory (see, for example, Ref. 25 and recent work in Ref. 26). On the other hand, with the nonrelativistic constraint $U_i(x) \equiv 1$ $(i = 1,2,3)$ that we impose, the phase structure of the compact theory will be quite different since, for instance, magnetic monopoles will not exist. However, the presence of vortices requires further investigations of the compact theory, which we will leave to future work. At present what is known from Ref. 3 is that the compact theory has a first-order phase transition in contrast to the second-order transition of the noncompact case. This very different phase structure indicates that nonperturbative features, such as vortices, are having a significant effect in distinguishing the two theories at strong coupling. In the present paper we show results for

both compact and noncompact gauge action. We find that the qualitative features do not change: the large flavor violations are present in either formulation at strong coupling.

ACKNOWLEDGMENTS

We are grateful to Joaquin Drut for numerous insightful questions and useful comments. Helpful communications were also received from Simon Hands and Timo Lähde. J.G. was supported by Rensselaer faculty development funds and by the U.S. Department of Energy, Office of Science, Office of High Energy Physics, Outstanding Junior Investigator program, Contract No. DE-FG02-08ER41575. A.S. and S.N. received support for this project from the New York State Interconnect Focus Center at Rensselaer.

APPENDIX: SIMULATION DETAILS

All of our results were obtained using hybrid Monte Carlo simulations with dynamical staggered fermions. This simulation method has been reviewed in the present context in Ref. 2. The mass in our simulations was $ma = 0.01$, where a is the lattice spacing. We have simulated on various sizes of lattices ($6^3 \times 8$, $8^3 \times 8$, $12^3 \times 8$, $16^3 \times 8$, and $24^3 \times 8$). We checked that the configurations were fully thermalized by comparing ordered and disordered starts.

*giedtj@rpi.edu
†askinner@skidmore.edu
‡nayaks@rpi.edu

[1] J. E. Drut and T. A. Lahde, Phys. Rev. B **79**, 241405(R) (2009); Phys. Rev. Lett. **102**, 026802 (2009).
[2] J. E. Drut and T. A. Lahde, Phys. Rev. B **79**, 165425 (2009).
[3] J. E. Drut, T. A. Lahde, and L. Suoranta, e-print arXiv:1002.1273 (to be published).
[4] W. Armour, S. Hands, and C. Strouthos, Phys. Rev. B **81**, 125105 (2010); e-print arXiv:0908.0118 (to be published); S. Hands and C. Strouthos, J. Phys. Conf. Ser. **150**, 042191 (2009); Phys. Rev. B **78**, 165423 (2008).
[5] D. V. Khveshchenko, Phys. Rev. Lett. **87**, 246802 (2001); E. V. Gorbar, V. P. Gusynin, V. A. Miransky, and I. A. Shovkovy, Phys. Rev. B **66**, 045108 (2002).
[6] D. T. Son, Phys. Rev. B **75**, 235423 (2007).
[7] J. E. Drut and D. T. Son, Phys. Rev. B **77**, 075115 (2008).
[8] D. Chakrabarti, S. Hands, and A. Rago, J. High Energy Phys. 06 (2009) 060.
[9] H. Neuberger, Phys. Lett. B **417**, 141 (1998).
[10] Y. Zhang, Y.-W. Tan, H. L. Stormer, and P. Kim, Nature (London) **438**, 201 (2005).
[11] J. B. Kogut and L. Susskind, Phys. Rev. D **11**, 395 (1975); L. Susskind, *ibid.* **16**, 3031 (1977); H. S. Sharatchandra, H. J. Thun, and P. Weisz, Nucl. Phys. B **192**, 205 (1981).
[12] This is analogous to the four flavors that appear in the 3 + 1-dimensional staggered formulation of lattice quantum chromodynamics.
[13] M. F. L. Golterman and J. Smit, Nucl. Phys. B **245**, 61 (1984).
[14] H. Kluberg-Stern, A. Morel, O. Napoly, and B. Petersson, Nucl. Phys. B **220**, 447 (1983).
[15] L. Del Debbio, S. Hands, and J. Mehegan (UKQCD Collaboration), Nucl. Phys. B **502**, 269 (1997).
[16] C. Davies, E. Follana, A. Gray, G. Lepage, Q. Mason, M. Nobes, J. Shigetmitsu, H. Trottier, M. Wingate, C. Aubin, C. Bernard, T. Burch, C. Detar, S. Gottlieb, E. Gregory, U. Heller, J. Hetrick, J. Osborn, R. Sugar, D. Toussaint, M. Dipierro, A. Elkhadra, A. Kronfeld, P. Mackenzie, D. Menscher, J. Simone (HPQCD Collaboration), Phys. Rev. Lett. **92**, 022001 (2004).
[17] C. DeTar and S. Gottleib, Physics Today **57**(2), 45 (2004).
[18] C. Bernard, T. Blum, T. A. DeGrand, C. DeTar, S. Gottlieb, U. M. Heller, J. E. Hetrick, C. McNeile, K. Rummukainen, B. Sugar, and D. Toussaint (MILC Collaboration), Phys. Rev. D **58**, 014503 (1998).
[19] E. Follana, Q. Mason, C. Davies, K. Hornbostel, G. Lepage, J. Shigemitsu, H. Trottier, and K. Wong (HPQCD Collaboration and UKQCD Collaboration), Phys. Rev. D **75**, 054502 (2007).
[20] S. Durr, C. Hoelbling, and U. Wenger, Phys. Rev. D **70**, 094502 (2004).
[21] G. P. Lepage and P. B. Mackenzie, Phys. Rev. D **48**, 2250 (1993).
[22] S. Naik, Nucl. Phys. B **316**, 238 (1989).
[23] T. Banks and A. Casher, Nucl. Phys. B **169**, 103 (1980).
[24] C. Morningstar and M. J. Peardon, Phys. Rev. D **69**, 054501 (2004).
[25] J. B. Kogut and E. Dagotto, Phys. Rev. Lett. **59**, 617 (1987).
[26] J. B. Kogut and C. G. Strouthos, Phys. Rev. D **67**, 034504 (2003).